

The Crystal Structure of $\text{La}_3\text{Mo}_{4.33}\text{Al}_{0.67}\text{O}_{14}$ and the Electronic Structure of $\text{La}_3\text{Mo}_4\text{XO}_{14}$ ($\text{X} = \text{Si}; \text{Mo}_{1/3}\text{Al}_{2/3}; \text{Al}_{1/2}\text{V}_{1/2}$)

W. H. MCCARROLL* AND K. PODEJKO

Chemistry Department, Rider College, Lawrenceville, New Jersey 08648

A. K. CHEETHAM* AND D. M. THOMAS

Chemical Crystallographic Laboratory, Oxford University, Oxford OX1 3PD, England

AND F. J. DISALVO

AT&T Bell Laboratories, Murray Hill, New Jersey 07974

Received March 18, 1985; in revised form September 3, 1985

Black needles of $\text{La}_3\text{Mo}_{4.33}\text{Al}_{0.67}\text{O}_{14}$ were prepared by electrolytic reduction at 1100°C of a melt containing Na_2MoO_4 , MoO_3 , and La_2O_3 held in an alumina crucible. The compound is isomorphous with $\text{La}_3\text{Mo}_4\text{SiO}_{14}$, crystallizing in space group $Pnma$ with $a = 17.750(3)$ Å, $b = 5.6600(9)$ Å, $c = 11.070(2)$ Å, $V = 1112.1(6)$ Å³, and $Z = 4$. The structure was refined by full-matrix least squares to $R_F = 3.43\%$, $R_{WF} = 3.45\%$, with 1912 independent reflections. As in $\text{La}_3\text{Mo}_4\text{SiO}_{14}$, the structure contains Mo_3O_{13} clusters and chains of edge-sharing MoO_6 octahedra with alternately short (2.535 Å) and long (3.167 Å) Mo-Mo distances, but unlike $\text{La}_3\text{Mo}_4\text{SiO}_{14}$, the tetrahedral silicon is replaced by a random distribution of $\frac{1}{3}$ Mo and $\frac{2}{3}$ Al. Electrical conductivity measurements show that $\text{La}_3\text{Mo}_4\text{SiO}_{14}$ and $\text{La}_3\text{Mo}_4\text{Al}_{2/3}\text{Mo}_{1/3}\text{O}_{14}$ are both highly anisotropic semiconductors with the easy direction of conduction being parallel to the chain cluster units. Semiempirical bond length-bond strength calculations lead to the conclusion that the valences of the molybdenums in both the chains and the clusters are remarkably similar. This coupled with the observed diamagnetism of the silicon compound can best be explained in terms of an electronic band structure rather than a localized model. © 1986 Academic Press, Inc.

Introduction

Recently we reported the synthesis and structure of $\text{La}_3\text{Mo}_4\text{SiO}_{14}$ (1), an unusual compound that contains both trigonal clusters of bonded molybdenum atoms and slightly puckered chains of edge-sharing MoO_6 octahedra which have alternating long and short Mo-Mo distances of 2.55 and 3.13 Å, (see Fig. 1). The trigonal clus-

ters are separated from each other by Mo-Mo distances of about 3.08 Å and run parallel to the chains which in turn are connected to the clusters by corner-sharing oxygens. These chain-cluster units run parallel to the orthorhombic b axis and are separated from similar chain-cluster units by about 5.5 Å, suggesting that the physical properties of this compound should be highly anisotropic.

The compound was originally prepared by the electrolytic reduction at 1075-

* To whom correspondence should be addressed.

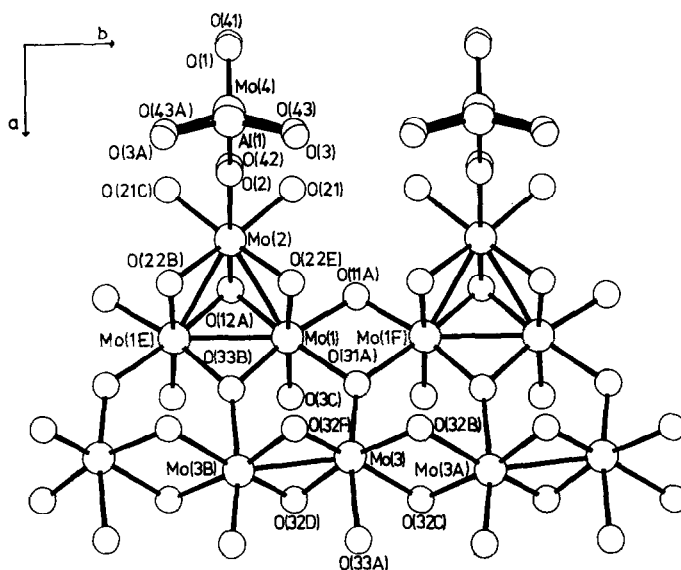


FIG. 1. Mo-O and Al,Mo-O units in $\text{La}_3\text{Mo}_4\text{Al}_{2/3}\text{Mo}_{1/3}\text{O}_{14}$.

1100°C of a melt containing Na_2MoO_4 , MoO_3 , and La_2O_3 , having a molar ratio of 3.00:3.00:1.00. The crystalline product grows out from the platinum cathode in the form of thin black needles or laminates, 1 to 3 mm long. The composition obtained depends upon the type of crucible used to contain the melt; a silica crucible produces $\text{La}_3\text{Mo}_4\text{SiO}_{14}$, a porcelain crucible yields a similar compound containing both silicon and aluminum, while the use of a high-density alumina crucible gives, in a much smaller yield, a product that has a slightly larger unit cell than $\text{La}_3\text{Mo}_4\text{SiO}_{14}$ and was presumed to be $\text{La}_3\text{Mo}_4\text{AlO}_{14}$.

The average oxidation state of molybdenum in $\text{La}_3\text{Mo}_4\text{SiO}_{14}$ is 3.75, equivalent to nine d electrons per formula unit. The trigonal cluster of Mo found in this compound is of the Mo_3O_{13} type, formed by edge-sharing MoO_6 octahedra; it is also found in $\text{Zn}_2\text{Mo}_3\text{O}_8$, $\text{LiZn}_2\text{Mo}_3\text{O}_8$, and $\text{Zn}_3\text{Mo}_3\text{O}_8$ (2-4). Approximate molecular orbital calculations have shown (5) that such clusters should be most stable for six electrons but are capable of accommodating up to eight electrons. Chains of molybdenum(IV) atoms, with al-

ternating long and short distances, are observed in MoO_2 (6), while similar chains of Mo(V) are probable in CrMoO_4 (7, 8). Thus, there appeared two plausible arrangements of the electrons in $\text{La}_3\text{Mo}_4\text{SiO}_{14}$ on the basis of a localized model: (1) seven electrons in the cluster and two per molybdenum in the chain or (2) eight electrons in the cluster and one per chain molybdenum.

In the belief that the crystals prepared in the alumina crucible were $\text{La}_3\text{Mo}_4\text{AlO}_{14}$ and would therefore contain only eight d electrons per formula unit, a complete single-crystal X-ray diffraction study was initiated with the expectation that any differences observed in the Mo-Mo distances in this compound and the silicon analog could be correlated with the preferred electron distribution. In fact, it was found that aluminum does not wholly replace silicon in the tetrahedral sites but rather, there is a statistical occupancy of this position by aluminum and molybdenum. The correct formula is $\text{La}_3\text{Mo}_4\text{Al}_{2/3}\text{Mo}_{1/3}\text{O}_{14}$. In addition, a study of the electrical and magnetic properties of these compounds was undertaken, as well as an examination of the possibility of con-

trolled valence variation of molybdenum by isomorphous replacement of silicon using classical solid state reactions.

Experimental

Synthesis. Single-crystal specimens of $\text{La}_3\text{Mo}_4\text{XO}_{14}$ type compounds were prepared by fused salt electrolysis at 1075°C of a melt formed from a mixture of Na_2MoO_4 , MoO_3 , and La_2O_3 in a molar ratio 3.00:3.00:1.00. The tetrahedral X atom is abstracted from the crucible used to contain the melt. $\text{La}_3\text{Mo}_4\text{SiO}_{14}$ was prepared in a high-purity silica crucible while a high-density alumina (McDanel 998) crucible was used to prepare $\text{La}_3\text{Mo}_4\text{Al}_{2/3}\text{Mo}_{1/3}\text{O}_{14}$. A porcelain crucible produces a mixed Si,Al,Mo phase in which the tetrahedral site is about 80–90% occupied by Si. Typically, a 1 hr run at 50–100 mA/cm² current density will produce 50–100 mg of a purified silicon containing product in contrast to a few milligrams for those runs in alumina crucibles, even when aluminium oxide is added to the starting mixture. The best yields of the aluminium-rich compound were obtained in a slightly modified version of the cell used to prepare alkali molybdenum oxide bronzes described by Perloff and Wold (9)₁. Further details regarding experimental conditions and chemical purification are given elsewhere (1, 10). Even after chemical washing, the product is still not pure, being intermixed with small hexagonal plates of LaMo_2O_5 , and a further, tedious mechanical separation is necessary.

Chemical analysis. Because the yield of the purified aluminium compound was so small, no wet chemical analysis was carried out. However, X-ray emission analysis of 21 crystallites carried out in a JOEL 100CX TEMSCAN analytical electron microscope yielded $\text{La}/\text{Mo} = 0.70(2)$, which is in accord with the chemical formula $\text{La}_3\text{Mo}_{4.33}\text{Al}_{0.67}\text{O}_{14}$ (Theo. $\text{La}/\text{Mo} = 0.692$). Spectroscopic

analysis of all phases showed no other elements to be present above the 500-ppm level, other than those indicated by the chemical formula.

Electrical and magnetic measurements. Electrical conductivity was measured using a four-point probe method. Contacts were made using Englehard No. 16 silver paint for measurements along the needle axis (*b* axis). Attachment of contacts perpendicular to the needle axis proved much more difficult and was facilitated by using an epoxy silver paint which dried much more slowly but yielded higher resistance contacts. The magnetic susceptibilities of the silicon and silicon–aluminum compounds were measured using the Faraday method. The experimental details have been described elsewhere (11).

Structure determination crystal data. $\text{La}_3\text{Mo}_4\text{Al}_{2/3}\text{Mo}_{1/3}\text{O}_{14}$, $M = 1074.4$ g, orthorhombic, $a = 17.750(3)$ Å, $b = 5.6600(9)$ Å, $c = 11.070(2)$ Å, space group *Pnma* (No. 62), $V = 1112.1(6)$ Å³, $\text{MoK}\alpha$ radiation (graphite monochromator), $\lambda = 0.71069$ Å, $\mu(\text{MoK}\alpha) = 161.9$ cm⁻¹, $D_{\text{calc}} = 6.416$ g/cm³, $Z = 4$.

Experimental details. The crystal selected for data collection was of dimensions ca. $(0.3 \times 0.05 \times 0.05)$ mm³. Diffracted intensities were collected for $0.0^\circ \leq \theta \leq 36.0^\circ$ on an Enraf-Nonius CAD-4 automated diffractometer. 4200 intensities were collected of which 226 were rejected as systematically absent. After merging equivalent reflections, 2834 unique intensities were obtained, but only 1912 with $I > 3\sigma(I)$ were used in refinement, where $\sigma(I)$ is the estimated standard deviation based on counting statistics. All data were corrected for Lorentz, polarization, X-ray absorption (empirical correction), and extinction effects. Anomalous dispersion corrections were applied to all atoms. A Chebyshev weighting scheme with three parameters was applied and 89 least-squares parameters were used in the final cycles of refine-

ment. Initial positional parameters were those of $\text{La}_3\text{Mo}_4\text{SiO}_{14}$. The tetrahedral site was initially assumed to be occupied entirely by Al, but although the refinement proceeded smoothly, the AlO_4 tetrahedra distorted unrealistically and the difference Fourier map indicated the presence of an atom at the tetrahedral site having approximately 22 electrons. Since spectroscopic analysis showed no metallic elements other than La, Mo, and Al to be present except in trace quantities, and the X-ray emission analysis indicated that $\text{La}/\text{Mo} = 0.70$, the occupancy of the tetrahedral site was then taken to be $\frac{2}{3}$ Al and $\frac{1}{3}$ Mo. The AlO_4 and MoO_4 tetrahedra were given soft constraints on the T–O bond distances at 1.74(1) Å and 1.79(1) Å, respectively (Fig. 2). The refinement converged at $R_F(R_{WF}) = 0.0343$ (0.0345). No abnormal features were observed in the difference Fourier (all peaks less than $3 \text{ e}\text{\AA}^{-3}$). After the refinement had converged, the validity of the tetrahedral site occupancy was confirmed by allowing the occupancy factors of Al(1) and Mo(4) to refine, their sum being constrained to 1.0; the refined values were 0.692(4) and 0.308(4), respectively.

Due to poor resolution in the area of the tetrahedral site, individual terms in the anti-

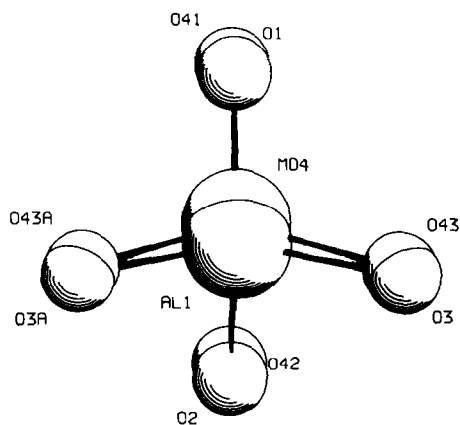


FIG. 2. Superposed MoO_4 and AlO_4 units at the tetrahedral site in $\text{La}_3\text{Mo}_4\text{Al}_{2/3}\text{Mo}_{1/3}\text{O}_{14}$.

TABLE I
ATOMIC POSITIONAL PARAMETERS (FRACTIONAL COORDINATES) WITH ESTIMATED STANDARD DEVIATIONS IN PARENTHESES FOR $\text{La}_3\text{Mo}_4\text{Al}_{2/3}\text{Mo}_{1/3}\text{O}_{14}$

Atom	x	y	z
La(1)	0.33565(4)	0.25000	0.13199(6)
La(2)	0.34657(4)	0.25000	0.49908(6)
La(3)	0.53414(4)	0.25000	0.69746(8)
Mo(1)	0.33906(3)	0.02356(10)	0.82069(6)
Mo(2)	0.21638(5)	0.25000	0.86281(9)
Mo(3)	0.50834(5)	0.2219(7)	0.00788(11)
Mo(4)	0.0548(5)	0.25000	0.0968(8)
Al(1)	0.0662(8)	0.25000	0.1114(15)
O(1)	-0.0246(7)	0.25000	0.0549(12)
O(2)	0.1318(9)	0.25000	0.9949(15)
O(3)	0.0850(18)	-0.0149(35)	0.1859(16)
O(11)	0.2890(5)	0.75000	0.7446(8)
O(12)	-0.2206(4)	0.25000	0.7918(7)
O(21)	0.1526(3)	-0.0001(10)	0.8023(5)
O(22)	-0.2709(3)	0.5070(11)	0.0339(5)
O(31)	-0.0999(5)	0.75000	0.5994(8)
O(32)	0.0446(3)	0.0010(12)	0.6112(6)
O(33)	0.0946(5)	0.75000	0.4096(8)
O(41)	-0.0304(10)	0.25000	0.0120(22)
O(42)	0.1241(15)	0.25000	0.9792(23)
O(43)	0.0809(36)	-0.0084(72)	0.1812(53)

sotropic thermal parameters for Al(1) and Mo(4) were constrained to the same values, as were the isotropic parameters of all oxygen atoms in the AlO_4 and MoO_4 tetrahedra (i.e., O(1), O(2), O(3), O(41), O(42), O(43)). Table I lists the atomic parameters and their estimated standard deviations. Table II lists their thermal parameters. Selected interatomic distances are given in Table III, and selected bond angles are given in Table IV.

Solid state synthesis. All reagents used in the solid state synthesis were of reagent grade or better with the exception of MoO_2 , obtained from ROC/RIC, which had a stated purity of 99.9%. Reactants were weighed out to the nearest milligram, the total charge usually being 5 g, mixed by grinding in an agate mortar, pressed into pellets (10,000 psi), and sealed in evacuated silica capsules at 30 Torr. Typically sam-

TABLE II
THERMAL PARAMETERS FOR $\text{La}_3\text{Mo}_4\text{Al}_{2/3}\text{Mo}_{1/3}\text{O}_{14}$

Atom	$U(11)$	$U(22)$	$U(33)$	$U(23)$	$U(13)$	$U(12)$
La(1)	0.0058(2)	0.0091(3)	0.0052(2)	0.0000	-0.0001(2)	0.0000
La(2)	0.0071(2)	0.0099(3)	0.0062(2)	0.0000	-0.0002(2)	0.0000
La(3)	0.0044(2)	0.0148(3)	0.0215(4)	0.0000	0.0006(2)	0.0000
Mo(1)	0.0037(2)	0.0052(2)	0.0050(2)	-0.0007(2)	0.0004(2)	0.0004(2)
Mo(2)	0.0034(3)	0.0064(4)	0.0049(3)	0.0000	-0.0001(3)	0.0000
Mo(3)	0.0044(3)	0.0075(21)	0.0076(4)	0.0000	0.0005(3)	0.0000
Mo(4)	0.0316(27)	0.0124(10)	0.0134(23)	0.0000	-0.0019(17)	0.0000
Al(1)	0.0316(27)	0.0124(10)	0.0134(23)	0.0000	-0.0019(17)	0.0000
$U(\text{iso})$						
O(1)	0.0122(11)					
O(2)	0.0122(11)					
O(3)	0.0122(11)					
O(11)	0.0090(14)					
O(12)	0.0063(13)					
O(21)	0.0106(10)					
O(22)	0.0065(9)					
O(31)	0.0081(14)					
O(32)	0.0138(11)					
O(33)	0.0085(14)					
O(41)	0.0122(11)					
O(42)	0.0122(11)					
O(43)	0.0122(11)					

ples were heated at 700°C for 48 hr, then at 1000°C, and finally at 1200°C for similar periods with samples being reground and re-pelleted before each temperature increase. Care was taken to remove the surface coating after each firing to minimize the addition of silica to the reaction mix.

Results and Discussion

$\text{La}_3\text{Mo}_4\text{SiO}_{14}$ and $\text{La}_3\text{Mo}_4\text{Al}_{2/3}\text{Mo}_{1/3}\text{O}_{14}$ are clearly isomorphous, the only difference being that silicon has been replaced by a statistical distribution of molybdenum and aluminium in the tetrahedral site. A comparison of pertinent Mo-Mo distances in the two compounds (Table V) shows no marked differences, suggesting that the d electron distributions between the chain and cluster are the same in both compounds. The molybdenum in the tetrahe-

dral site is hexavalent in $\text{La}_3\text{Mo}_4\text{Al}_{2/3}\text{Mo}_{1/3}\text{O}_{14}$ and the average valence for this site remains four.

This conclusion is supported by infrared spectra data and the results of solid state syntheses. A series of solid state reactions were performed in which the composition was carefully controlled to confirm that elements other than molybdenum can replace silicon. The results of these runs, which are summarized in Table VI, clearly show that aluminum must be present if silicon is absent and that vanadium can replace molybdenum to yield $\text{La}_3\text{Mo}_4\text{Al}_{1/2}\text{V}_{1/2}\text{O}_{14}$. The fact that neither germanium or titanium would replace silicon in this structure was surprising, but these reactions produce what appear to be previously unreported phases. The presence of a small amount of LaAlO_3 in the $\text{La}_3\text{Mo}_4\text{Al}_{2/3}\text{Mo}_{1/3}\text{O}_{14}$ product is ascribed to the formation of the silicon

TABLE III
SELECTED INTERATOMIC DISTANCES IN ANGSTROMS
FOR $\text{La}_3\text{Mo}_4\text{Al}_{23}\text{Mo}_{13}\text{O}_{14}$ WITH ESTIMATED
STANDARD DEVIATIONS IN PARENTHESES

La(1)–O(11B)	2.540(9)	Mo(1)–Mo(1E)	2.563(1)
O(21B)	2.366(6)	Mo(1F)	3.097(1)
O(21D)	2.366(6)	Mo(2)	2.570(1)
O(22A)	2.566(6)	O(3C)	2.01(2) ^a
O(22D)	2.566(6)	O(11A)	1.974(5)
O(32C)	2.567(6)	O(12A)	2.077(6)
O(32D)	2.567(6)	O(22E)	2.016(5)
O(33A)	2.755(9)	O(31A)	2.087(6)
La(2)–O(1A)	2.365(12)	O(33B)	2.000(6)
O(2)	2.856(2)	O(43C)	2.10(4) ^a
O(2A)	2.856(2)	Mo(2)–O(2)	2.10(2) ^a
O(3A)	2.74(3)	O(12A)	2.044(8)
O(3C)	2.74(3)	O(21)	1.932(6)
O(12A)	2.604(8)	O(21C)	1.932(6)
O(21B)	2.597(6)	O(22B)	2.035(6)
O(21D)	2.597(6)	O(22E)	2.035(6)
O(22C)	2.569(6)	O(42)	2.08(2) ^a
O(22F)	2.569(6)	Mo(3)–Mo(3A)	3.167(8)
O(41A)	2.187(17)	Mo(3B)	2.535(8)
O(42)	2.886(6)	O(31A)	1.921(8)
O(42A)	2.886(6)	O(32B)	2.147(7)
O(43A)	2.76(6)	O(32C)	2.165(7)
O(43C)	2.76(6)	O(32D)	1.945(7)
La(3)–O(1)	2.98(1)	O(32F)	1.927(7)
O(2B)	2.75(2)	O(33A)	2.132(8)
O(3A)	2.50(2)	Mo(4)–O(41)	1.779(9)
O(3C)	2.50(2)	O(42A)	1.792(10)
O(21A)	2.535(6)	O(31A)	1.921(8)
O(21E)	2.535(6)	O(43)	1.796(9)
O(32A)	2.551(6)	O(43B)	1.796(9)
O(32E)	2.551(6)	Al(1)–O(1)	1.728(9)
O(41)	2.59(3)	O(2A)	1.739(9)
O(42B)	2.52(3)	O(3)	1.743(8)
O(43A)	2.46(4)	O(3B)	1.743(8)
O(43C)	2.46(4)		

^a The Mo,Al disorder in the tetrahedral site led to occupancy factors for O(3C) and O(2) of 0.7 and of 0.3 for O(43C) and O(42).

compound on the surface of the pellet due to reaction with the silica capsule. Indeed, the X-ray powder diffraction photograph of the surface coating of a very fine matte of tiny needles found on the 1200°C run showed them to be the silicon-rich compound, while the bulk material was clearly the title compound.

The IR spectra of the various products are shown in Fig. 3. Features at energies below $\sim 750\text{ cm}^{-1}$ can be ascribed to octahedral Mo. The strong peaks in the vicinity of 965, 930, and 855 cm^{-1} found for the Si-containing compounds are absent in the

spectra of the other materials. These peaks should therefore be ascribed to Si–O vibrations. The weak peak or shoulder at 805 cm^{-1} found in the spectrum of the title compound would be consistent with the presence of tetrahedrally coordinated molybdenum(VI). Strong peaks in this vicinity are found in the spectra of many scheelite type molybdates where molybdenum is also found in slightly distorted tetrahedra (12). The very small shoulder at 803 cm^{-1} in spectrum b confirms the incorporation of a small amount of Mo into this compound also, while the peak at 822 cm^{-1} found in the spectrum of the vanadium compound is typical of VO_4 groups (12). The very weak peaks around 945 and 930 cm^{-1} in spectra c and d are probably due to Al–O vibrations; a third peak, expected in the 800–900 cm^{-1} region, may be hidden under the strong Mo–O and V–O absorptions.

The temperature dependence of the electrical resistivities of both $\text{La}_3\text{Mo}_4\text{SiO}_{14}$ and the title compound, measured along the *b* axis (needle axis), are shown in Fig. 4. Both compounds are semiconductors with similar activation energies of 0.065 and 0.050 eV, respectively. Because of uncertainties in defining crystal dimensions relative to the contacts, the absolute values of the resistivities are probably no better than $\pm 30\%$. Qualitative measurements of the sign of the Seebeck coefficient in the room temperature region indicate that the majority carriers are electrons. Measurement of the resistance perpendicular to the needle axis proved much more difficult since the crystals are typically no more than 0.03–0.05 mm thick and are easily broken when contacts are applied. Further it is difficult to control with certainty the direction of the current flow. Although we were successful in making ohmic contacts on $\text{La}_3\text{Mo}_4\text{SiO}_{14}$ crystals in two instances, the crystals fragmented on cooling. Thus, only room-temperature data is available for this direction; this shows a resistivity measured perpen-

TABLE IV
SELECTED BOND ANGLES IN DEGREES FOR $\text{La}_3\text{Mo}_4\text{Al}_{2/3}\text{Mo}_{1/3}\text{O}_{14}$

Mo(1E)–Mo(2)–Mo(1)	59.84(3)	O(31A)–Mo(3)–O(32B)	91.6(3)
Mo(2)–Mo(1E)–Mo(1)	60.08(2)	O(32C)	90.6(3)
Mo(1E)–Mo(1)–Mo(2)	60.08(2)	O(33A)	170.9(2)
Mo(3B)–Mo(3)–Mo(3A)	165.97(8)	O(32D)	97.6(3)
O(22E)–Mo(1)–O(11A)	91.9(3)	O(32F)	98.8(3)
O(31A)	86.5(3)	O(32B)–Mo(3)–O(32C)	85.5(3)
O(3C)	173.4(7)	O(33A)	81.0(2)
O(33B)	86.5(3)	O(32D)	168.4(2)
O(12A)	101.6(3)	O(32F)	87.3(4)
O(11A)–Mo(1)–O(31A)	80.4(2)	O(32C)–Mo(3)–O(33A)	83.6(2)
O(3C)	88.0(5)	O(32D)	87.4(4)
O(33B)	167.9(2)	O(32F)	168.4(2)
O(12A)	89.9(2)	O(33A)–Mo(3)–O(32D)	89.2(3)
O(31A)–Mo(1)–O(3C)	87.0(7)	O(32F)	86.2(3)
O(33B)	87.8(2)	O(32D)–Mo(3)–O(32F)	86.2(3)
O(12A)	167.6(2)	O(41)–Mo(4)–O(43)	120(1)
O(3C)–Mo(1)–O(33B)	89.2(5)	O(42A)	102(2)
O(12A)	85.0(7)	O(43B)	120(1)
O(33B)–Mo(1)–O(12A)	101.5(2)	O(43)–Mo(4)–O(42A)	102(2)
O(2)–Mo(2)–O(21)	79.8(4)	O(43B)	109(3)
O(22E)	87.0(4)	O(42A)–Mo(4)–O(43B)	102(2)
O(12A)	167.4(5)	O(1)–Al(1)–O(3)	110(1)
O(22B)	87.0(4)	O(2A)	111(1)
O(21C)	79.8(4)	O(3B)	110(1)
O(21)–Mo(2)–O(22E)	88.8(2)	O(3)–Al(1)–O(2A)	103(1)
O(12A)	91.7(2)	O(3B)	119(2)
O(22B)	165.7(2)	O(2A)–Al(1)–O(3B)	103(1)
O(21C)	94.2(3)		
O(22E)–Mo(2)–O(12A)	102.1(2)		
O(22B)	85.1(3)		
O(21C)	165.7(2)		
O(12A)–Mo(2)–O(22B)	102.1(2)		
O(21C)	91.7(2)		
O(22B)–Mo(2)–O(21C)	88.8(2)		

TABLE V
COMPARISON OF Mo–Mo BOND DISTANCES AND ANGLES IN $\text{La}_3\text{Mo}_4\text{SiO}_{14}$ AND $\text{La}_3\text{Mo}_4\text{Al}_{2/3}\text{Mo}_{1/3}\text{O}_{14}$

Distance or angle	$\text{La}_3\text{Mo}_4\text{SiO}_{14}$	$\text{La}_3\text{Mo}_4\text{Al}_{2/3}\text{Mo}_{1/3}\text{O}_{14}$
Mo(1)–Mo(1E)	2.562(1) Å	2.563(1) Å
Mo(1)–Mo(2)	2.551(1) Å	2.570(1) Å
Mo(1)–Mo(1F)	3.081(1) Å	3.097(1) Å
Mo(3)–Mo(3A)	3.128(11) Å	3.167(8) Å
Mo(3)–Mo(3B)	2.549(11) Å	2.535(8) Å
Mo(1E)–Mo(2)–Mo(1)	60.3(0)°	59.84(3)°
Mo(2E)–Mo(1E)–Mo(1)	59.8(0)°	60.08(2)°
Mo(1E)–Mo(1)–Mo(2)	59.8(0)°	60.08(2)°
Mo(3B)–Mo(3)–Mo(3A)	168.1(5)°	165.97(8)°

dicular to b and parallel to a of $35 \pm 25 \Omega\text{-cm}$, as compared to $0.05 \pm 0.02 \Omega\text{-cm}$ when measured along the b axis. This striking difference supports the hypothesis that the easy direction of conduction should be parallel to the chain or chain-cluster units.

Magnetic susceptibility measurements over the range from 298 to 4 K were made on randomly oriented crystals of both $\text{La}_3\text{Mo}_4\text{SiO}_{14}$ and $\text{La}_3\text{Mo}_4\text{Si}_x(\text{Al}_{2/3}\text{Mo}_{1/3})_{1-x}\text{O}_{14}$. The susceptibility of $\text{La}_3\text{Mo}_4\text{SiO}_{14}$ (Fig. 5) fits the simple Curie-Weiss expression: $\chi_g = \chi_0 + C_g/(T + \theta)$ with $\chi_0 = +0.300 \times 10^{-6}$

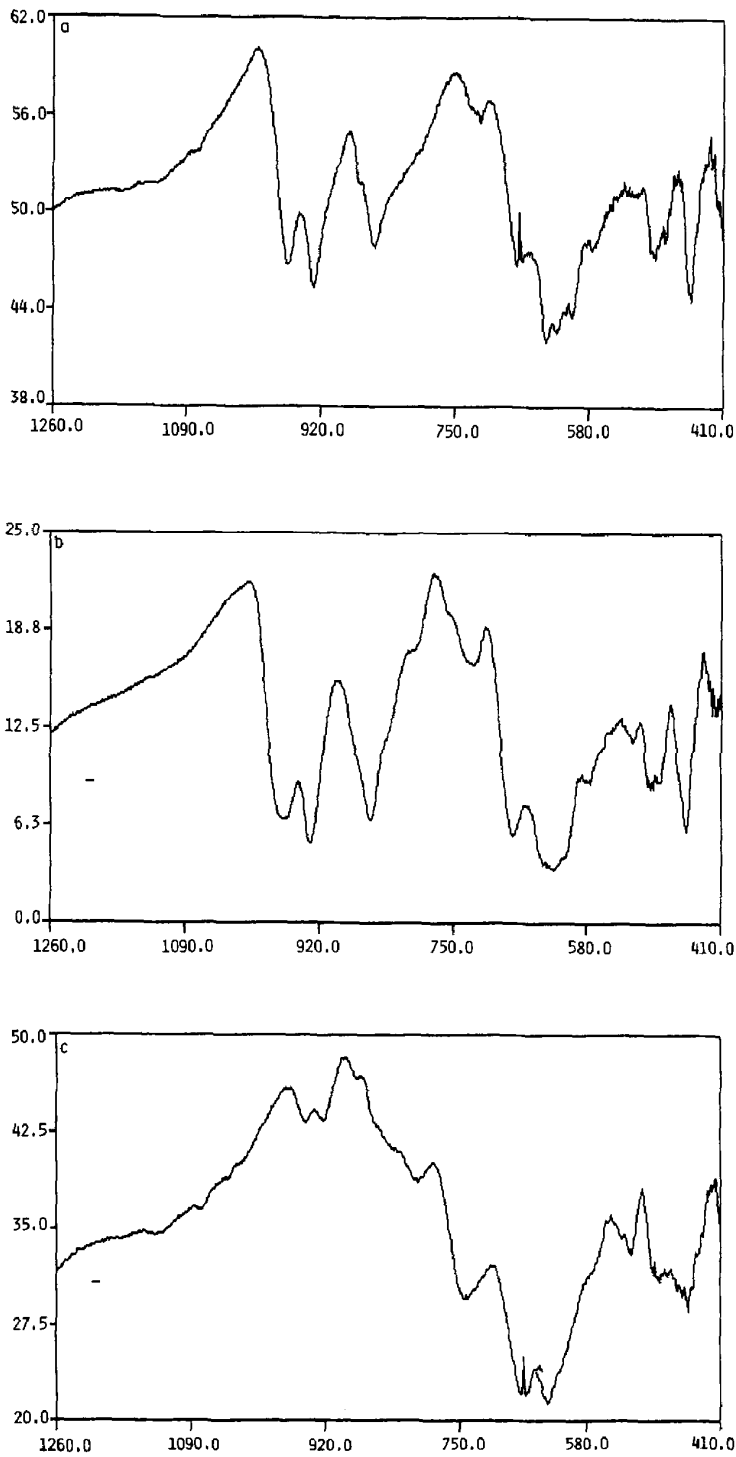


FIG. 3. Infrared spectra for various $\text{La}_3\text{Mo}_4\text{XO}_{14}$ phases: (a) $X = \text{Si}$; (b) $X = \text{Si,Al}$; (c) $X = \text{Al}_{2/3}\text{Mo}_{1/3}$; (d) $X = \text{V}_{1/2}\text{Al}_{1/2}$.

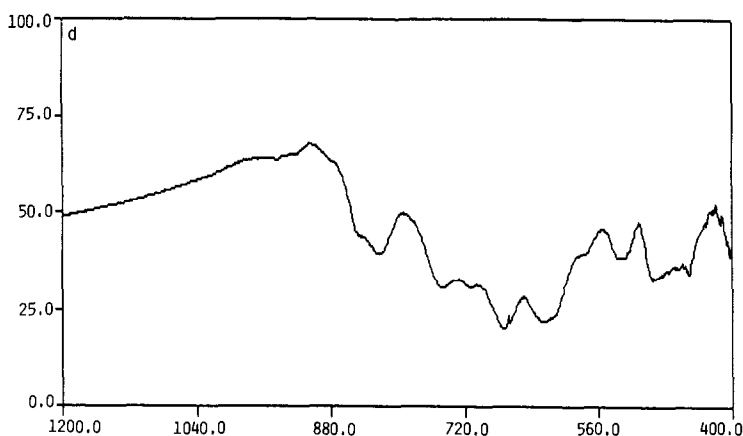


FIG. 3—Continued.

emu/g ($\pm 3\%$), $C_g = 11.9 \times 10^{-6}$ emu-K/g and $\theta = 4.5$ K. The fit is for 200 data points over the interval 6.0–120 K with a standard deviation of 0.45%. The increasing susceptibility at low temperature is 30 times too small to be due to a $S = \frac{1}{2}$, $g = 2$ moment on the Mo cluster. The increase is most likely due to paramagnetic impurities such as Fe (approximately 150 ppm Fe, assuming $S = 2$, $g = 2$, which is within the range of typical impurity levels of these samples). Since

the material is known to be a semiconductor, the weakly paramagnetic value of χ_0 is due to Van Vleck paramagnetism. There was an insufficient quantity of crystals of the title compound, of suitable purity, to justify making a similar measurement for this material.

If one looks at the structure in terms of isolated triangular clusters of molybdenum and chains of molybdenum which are alternately bonding, the assignment of eight electrons to the cluster and one bonding electron to each Mo in the chain would appear to offer a rational explanation for the observed magnetic properties. The molybdenum–molybdenum bond distances in the clusters are quite close to those found by McCarley and Torardi (3, 4) in the seven and eight electron clusters of $\text{LiZn}_2\text{Mo}_3\text{O}_8$ (2.578 Å) and $\text{Zn}_3\text{Mo}_3\text{O}_8$ (2.580 Å). Although the Mo–Mo bonding distances in the chains (See Table V) are somewhat shorter than might be expected for single bonds, none the less similar distances have been found in pentavalent molybdenum complexes. For instance, the Mo–Mo distance in $\text{BaMo}_2\text{O}_4(\text{C}_2\text{O}_4) \cdot 5\text{H}_2\text{O}$ is 2.541 Å (13) while that in $\text{Mo}_2\text{O}_3\text{Cl}(\text{CH}_3\text{COO})_3$ is 2.601 Å (14). Further, Koch and Lincoln (15) have reported the synthesis of an oxopyrazolyborate complex of pentavalent

TABLE VI

RESULTS OF SOLID STATE REACTIONS AT 1200°C

Nominal Sample Composition	Comments
$\text{La}_3\text{Mo}_4\text{SiO}_{14}$	XRDP ^a identical with single crystal material.
$\text{La}_3\text{Mo}_4\text{O}_{14}$	XRDP shows $\text{La}_3\text{Mo}_3\text{O}_{16}$ plus unidentified phases.
$\text{La}_3\text{Mo}_4\text{AlO}_{14}$	XRDP shows $\text{La}_3\text{Mo}_4\text{Al}_{2/3}\text{Mo}_{1/3}\text{O}_{14}$ plus several strong lines belonging to LaAlO_3 . Sample visually heterogeneous.
$\text{La}_3\text{Mo}_4\text{Al}_{2/3}\text{Mo}_{1/3}\text{O}_{14}$	XRDP shows $\text{La}_3\text{Mo}_4\text{Al}_{2/3}\text{Mo}_{1/3}\text{O}_{14}$ dominates. A few weak lines are strongest lines of LaAlO_3 . Sample visually homogeneous.
$\text{La}_3\text{Mo}_4\text{V}_{1/2}\text{Al}_{1/2}\text{O}_{14}$	XRDP is single phase with d spacing similar to those of (Al) compound. Sample is visually homogeneous.
$\text{La}_3\text{Mo}_4\text{GeO}_4$ $\text{La}_3\text{Mo}_4\text{TiO}_4$	XRDP cannot be identified. XRDP cannot be identified.

^a XRDP = X-ray diffraction pattern.

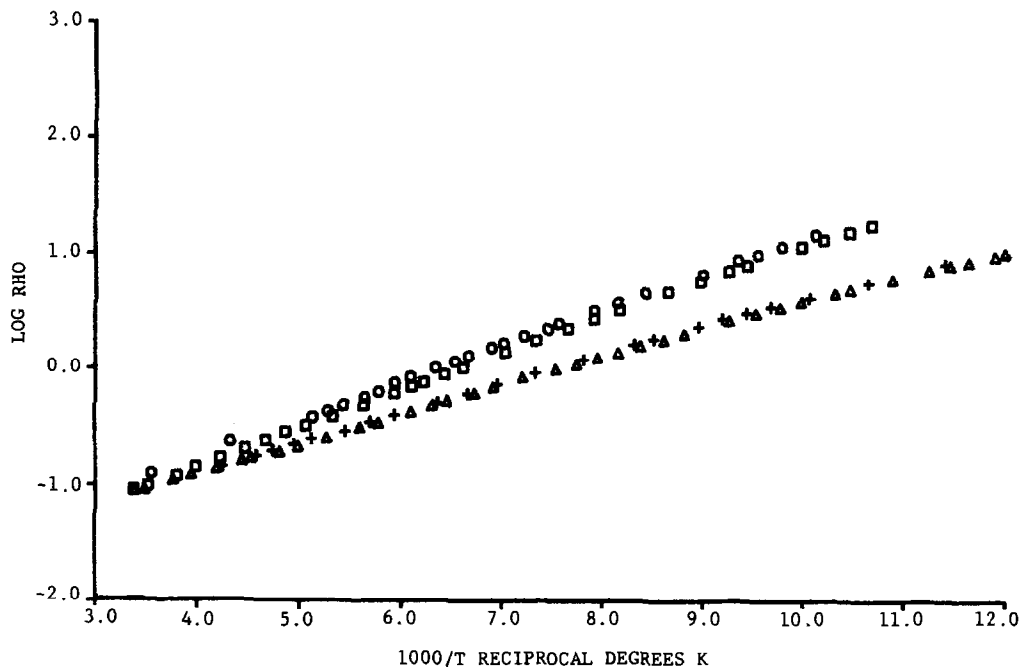


FIG. 4. Variation of $\log \rho$ with temperature for $\text{La}_3\text{Mo}_4\text{SiO}_{14}$ (+, Δ) and $\text{La}_3\text{Mo}_4\text{Al}_{2/3}\text{Mo}_{1/3}\text{O}_{14}$ (O, \square). Current passed parallel to orthorhombic b axis.

molybdenum which contains a tetrameric chain with alternating long and short Mo–Mo lengths in which the bonding distance is 2.553 Å.

However, if one calculates the average valences of the molybdenums in $\text{La}_3\text{Mo}_4\text{SiO}_{14}$ using the bond length–bond strength relationship given by Brown and Wu (16) for molybdenum–oxygen bonds, valences

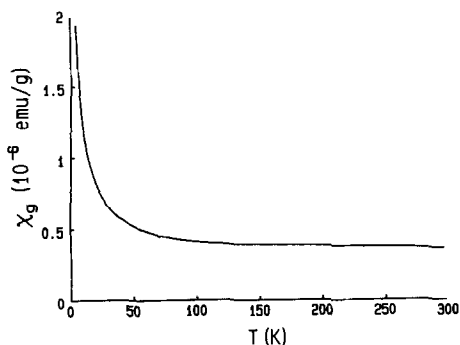


FIG. 5. Magnetic susceptibility vs temperature for $\text{La}_3\text{Mo}_4\text{SiO}_{14}$.

of 3.62, 4.05, and 3.84 are obtained for Mo(1), Mo(2), and Mo(3), respectively. Similar results of 3.79, 4.10, and 3.93 are obtained for the cluster and chain molybdenums in the aluminum compound. Such calculations are semiempirical and in part ignore the effects of valence and coordination geometry and as such should not be interpreted too literally. On the other hand they have been applied with a remarkable degree of success to a wide variety of complex molybdenum oxides in a number of different valence states (17–20). Indeed, deviations of the bond strength sum from the observed valence of more than 0.3 units are unusual. Since the observed differences based upon the 8 to 1 electron assignment between the cluster and chain are considerably larger than this, alternate distributions or models must be examined.

The average valence calculated from bond lengths for the cluster molybdenums in $\text{La}_3\text{Mo}_4\text{SiO}_{14}$ is 3.76 while that for the

chain molybdenums is 3.84. For the aluminum compound these values are 3.89 for the cluster molybdenums and 3.93 for those in the chain. The differences between the two are in part due to uncertainties in the positions of the oxygens in the aluminum compound which are involved in both tetrahedral and octahedral coordination (i.e., O(2) or O(42) and O(3) or O(43)). None the less the small differences between the valence sums for the chains and clusters in both compounds is noteworthy and is inconsistent with the assignment of 8 electrons per cluster and one electron per chain Mo. On the other hand, a localized picture of electron distribution also fails to account for the physical properties (i.e., no observed magnetic moment and a relatively high electrical conductivity along the chain axis) if the valences obtained from bond strength sums are used, since they are consistent with the assignment of 7 electrons per cluster and thus should result in a paramagnetic moment that would be observed in the susceptibility. It seems likely that such a localized description of the electronic states is incorrect and that a band model must be used to understand the properties of these materials.

Indeed many binary molybdenum oxides and at least some ternaries such as $\text{K}_{0.3}\text{MoO}_3$ are either small band gap semiconductors with reasonable electron (or hole) mobilities or are in fact metallic conductors. In the case of $\text{La}_3\text{Mo}_4\text{SiO}_{14}$ and $\text{La}_3\text{Mo}_{4.33}\text{Al}_{0.67}\text{O}_{14}$, there are 4 formula units per unit cell or 36 nonbonding d electrons to accommodate above the metal-oxygen bonding bands. Since each band can hold exactly two electrons per unit cell and since the material is semiconducting, these 36 electrons must fill a total of 18 bands. If the gap between the highest occupied band and the lowest unoccupied band is small, the temperature independent paramagnetism χ_0 , apparent near room temperature could arise from Van Vleck coupling of the 18

occupied Mo bands (which may or may not overlap) to the higher unoccupied Mo bands.

A band picture might also explain why both the cluster and the chain Mo-Mo distances are so similar as well as the fact that the chains and clusters are relatively close to one another.

The Mo-Mo angles in the chains of both $\text{La}_3\text{Mo}_4\text{SiO}_{14}$ and the title compound are remarkably similar to those in MoO_2 , the latter value being 172.6° . In this respect it would be tempting to apply the Goodenough model of electronic conduction in rutile-type oxides (21, 22) to this system. This would predict semiconducting behavior for a chain containing doubly bonded molybdenums providing that the bridging oxygens of the edge sharing MoO_6 octahedra could not form Mo-O π bonds as is the case here. However, it would appear that the highest occupied band in the system under consideration is one which must contain electrons from both the chains and clusters since the direction of easiest conduction lies parallel to the chain or more correctly, the chain-cluster unit.

Acknowledgments

W.H.M. and K.P. acknowledge the support of Research Corp. for the purchase of materials and supplies. We also thank Professor R. Herber of Rutgers University for recording the IR spectra.

References

1. R. W. BETTERIDGE, A. K. CHEETHAM, J. A. K. HOWARD, G. JAKUBICKI, AND W. H. MCCARROLL, *Inorg. Chem.* **23**, 737 (1984).
- 2a. W. H. MCCARROLL, L. KATZ, AND R. WARD, *J. Am. Chem. Soc.* **79**, 5410 (1957).
- 2b. G. B. ANSEL AND L. KATZ, *Acta Crystallogr.* **21**, 482 (1966).
3. C. C. TORARDI AND R. E. MCCARLEY, *Inorg. Chem.* **24**, 476 (1985).
4. C. C. TORARDI AND R. E. MCCARLEY, *J. Solid State Chem.* **37**, 393 (1981).
5. F. A. COTTON, *Inorg. Chem.* **3**, 1217 (1964).
6. B. J. BRANDT AND A. C. SKAPSKI, *Acta Chem. Scand.* **21**, 661 (1967).

7. J. DOUMERC, M. POUCHARD, AND P. HAGENMULLER, *C.R. Acad. Sci. Ser. C* **280**, 1397 (1975).
8. C. TENRET-NOEL, J. VERBIST, *J. Microsc. Spectrosc. Electron.* **1**, 255 (1977).
9. D. PERLOFF AND A. WOLD, *Phys. Chem. Solid. Suppl.* **1**, **28**, 361 (1967).
10. W. H. MCCARROLL, C. DARLING, AND G. JAKUBICKI, *J. Solid State Chem.* **48**, 189 (1983).
11. F. J. DISALVO AND J. V. WASZCZAK, *Phys. Rev. B* **23**, 457 (1981).
12. R. A. NYQUIST AND R. O. KAGE, "Infra Red Spectra of Inorganic Compounds," Academic Press, New York, 1971.
13. F. A. COTTON AND S. M. MOOREHOUSE, *Inorg. Chem.* **4**, 1377 (1965).
14. B. KAMENAR, M. PENAVIC, AND B. KORPARCOLIG, *J. Chem. Soc. Dalton Trans.*, 311 (1981).
15. S. A. KOCH AND S. LINCOLN, *Inorg. Chem.* **21**, 2904 (1982).
16. I. D. BROWN AND K. K. WU, *Acta Crystallogr. Ser. B* **32**, 1957 (1976).
17. J. C. J. BART, AND V., RAGAINI, *Inorg. Chem. Acta* **36**, 261 (1979).
18. R. E. MCCARLEY, K. H. LIU, P. H. EDWARDS, AND L. F. BROUGH, *J. Solid State Chem.* **57**, 17 (1985).
19. M. GHEDIRA, J. CHENAVAS, M. MAREZIO, AND J. MARCUS, *J. Solid State Chem.* **57**, 300 (1985).
20. C. C. TORARDI AND J. CALABRESE, *Inorg. Chem.* **23**, 3281 (1984).
21. J. B. GOODENOUGH, *J. Solid State Chem.* **3**, 490 (1971).
22. J. B. GOODENOUGH, "Progress in Solid State Chemistry" (H. Reiss, Ed.), Vol. 5, p. 344, Pergamon, Oxford, 1971.